JOURNAL OF SPACECRAFT AND ROCKETS
Vol. 42, No. 6, November–December 2005

Correlation of Double Star Anomalies with Space Environment

Jianwei Han,* Jianguo Huang,† Zhenxing Liu,‡ and Shijin Wang§
Chinese Academy of Sciences, Beijing 100080, People's Republic of China

From 27 July 2004 to 10 August 2004, TC-1 and TC-2 satellites suffered flux gate magnetometer resets, remote terminal stops, and a few other instrument anomalies more than 30 times during the short period. Convincing evidence is presented that internal discharges due to the enhancement of penetrating electron flux during this period led to the anomalies for both spacecraft. Although their orbits are much different, with the former being equatorial and the latter being polar, both of their various anomalies coincide with the enhancement of penetrating electron flux and are densely populated in the outer radiation belt. Integrated flux of electrons greater than 2 MeV experienced in orbit are in good agreement with the pattern of event occurrence. Although direct evidence is only available by identification of the breakdown sites and ground reproduction of the anomalies, the correlation of anomalies with space environment still provides evidence that internal discharges are probably to be blamed for the anomalies, which implies that the hazard is underestimated and that the protection is inadequate.

I. Introduction

SATELLITES TC-1 and TC-2, known together as Double Star, were designed, developed, and launched by the Chinese National Space Administration, with the mission of studying the solar effect on the Earth's environment in concert with ESA's cluster mission. The equatorial spacecraft TC-1 was launched 29 December 2003, running in an elliptical orbit of 555 × 78,051 km, inclined at 28 deg to the equator. This enables it to investigate the Earth's huge magnetic tail, the region where particles are accelerated toward the planet's magnetic pole by reconnection. The polar satellite TC-2 was launched 25 July 2004 into a 681 × 38,278 km polar orbit, concentrating on the physical processes taking place over the magnetic poles and the development of auroras.

Shortly after the launch of TC-2 satellite, both TC-1 and TC-2 suffered dense anomalies, which exhibited as a majority of flux gate magnetometer (FGM) resets and remote terminal (RT) stops accompanied by a few other instrument malfunctions. In general, the operational anomalies of spacecraft can be attributed to two factors: hardware and the space environment. Because the TC-1 satellite had been in normal operation since its launch before these anomalies occurred, the cause of hardware malfunctions can be eliminated. What is more important is that the two satellites with such different orbits encounter like problems simultaneously, for which the only reasonable explanation is that their anomalies are caused by a common factor, the space environment.

Most environment-induced spacecraft anomalies are related to single-event upsets, differential surface discharges, and internal discharges. Single-event upsets occur when a proton or heavy ion generates enough free carriers in a sensitive volume of a microelectronic device to cause the circuit to change state. Single-event upsets generally cause soft errors such that the circuit can be reset to its original state. Spacecraft anomalies due to single-event upsets usually take place when the vehicle encounters a large enhancement of high energetic protons and the error rate is very low. Differential surface charging is produced by interactions between satellite surfaces and space plasma, with different surface material components charged to different voltages. The voltage difference can cause large electrostatic discharge (ESD), which may burn out components or couple noises into sensitive electronic circuits or components. Differential surface charging in the space environment is reported to correlate best with the intensity of electrons with energies ≤50 keV (Refs. 1–4). Electrons with energies greater than 100 keV may penetrate beyond the spacecraft surface shield to produce internal charging. The penetrating electrons can become embedded inside dielectrics, such as thermal control blankets, cables, and printing circuit boards. These materials are usually poorly conductive so that the deposited charges build up until the local electric field exceeds the breakdown threshold of the material and an ESD occurs. Apart from the general detrimental effect of ESD, internal discharging is more threatening than surface discharging because the ESD occurs inside the spacecraft, and the coupling of noises is more direct and severe. Spacecraft anomalies induced by internal discharges generally correlate well with the enhancement of penetrating electrons in the Earth's outer radiation belt.[5–7]

The purpose of this paper is to correlate TC-1 and TC-2 anomalies with space environment data, discuss the possible mechanisms for their occurrences, and present according evidence.

II. Statistics of Anomalies

The statistics of the anomalies are listed in Table 1, with anomaly type (FGM reset or RT stop), the universal time, the moments of events relative to perigee, and orbital locations presented. In the column time relative to perigee, a negative sign indicates an inbound segment relative to perigee, and a positive sign indicates an outbound segment. In the column of L, the question mark indicates that the L value is too large to be reliable. The anomalous *SP* refers to anomalous pulse detected by the sun's pulse sensor. Moreover, a few other instrument anomalies are not included in Table 1. The pattern of anomaly occurrence exhibits the following characteristics:

1) The majority of anomalies occurred in the Earth's radiation belt ($L = 2 \sim 7$).

2) Among the anomalies, FGM resets and RT stops occurred simultaneously four times, with a percentage of nearly 13%.

3) For the TC-1 satellite, the anomalies were distributed in both the inbound and outbound segments relative to perigee; but for TC-2, nearly all of the events occurred in the outbound segment.

4) As for the distribution of the anomalies in magnetic local time (MLT), although TC-2's events were populated in the sector from local midnight to dawn, TC-1's events did not show any apparent pattern.

Received 26 November 2004; revision received 1 February 2005; accepted for publication 1 February 2005.

*Vice Director, Post Office Box 8701, Space Environment Prediction Center, Center for Space Science and Applied Research; jwhan@earth.sepc.ac.cn.

†Adjunct Professor, Post Office Box 8701, Space Environment Prediction Center, Center for Space Science and Applied Research; jghuang@earth.sepc.ac.cn.

‡Academician of Chinese Academy of Sciences, Post Office Box 8701, and Prime Scientist of Geospace Double Star Program, Laboratory for Space Weather, Center for Space Science and Applied Research.

§Director, Post Office Box 8701, Division of Space Environment Detection, Center for Space Science and Applied Research.

Table 1 Anomalies on TC-1 and TC-2 satellites

No.	Date	FGM reset time	RT stop time	Altitude, km	*L*, *Re*	Time relative to perigee, h	MLT, h
			TC-1				
1	27 July 2004	21:40:26	21:39:59	15,331.52	3.4	−1.02	6.13
		Anomalous SP					
2	29 July 2004	01:18:14		11,574.14	2.98	−0.77	6.67
3	29 July 2004	03:03:21		14,702.30	3.6	0.98	22.2
4	29 July 2004	03:09:37		16,276.82	3.86	1.08	22.4
5	30 July 2004	04:18:00		17,453.93	3.99	−1.17	5.72
6	30 July 2004	06:48:17		19,932.17	4.64	1.34	22.8
7	31 July 2004	09:42:33		12,857.82	4.29	0.86	21.7
8	3 Aug. 2004	18:11:50		12,710.20	3.2	0.85	6.10
9	6 Aug. 2004	03:01:03		18,883.56	4.3	1.26	22.3
10	7 Aug. 2004	04:45:51		54,369.6	1.9	−0.38	7.80
11	15 March 2004	15:14:25		70,884.61			10.0
12	23 Jan. 2004	07:32:06		78,932.25			13.8
			TC-2				
1	27 July 2004		18:35:08	18,802.92	4.18	1.50	2.7
2	28 July 2004		16:48:55	9,911.22	2.69	0.76	3.0
3	30 July 2004		14:54:29	12,202.47	2.92	0.93	2.4
4	31 July 2004		02:27:44	13,183.48	3.1	1.00	2.6
5	1 Aug. 2004	15:21:29		33,141.23	10.8	3.45	1.7
6	2 Aug. 2004	01:06:47	01:06:47	21,235.24	5.13	1.73	2.8
		Anomalous SP					
7	2 Aug. 2004	03:04:10		34,124.34	73.9	3.76	3.2
8	2 Aug. 2004	14:11:00		32,460.51	10.9		1.5
9	3 Aug. 2004	05:10:32		37,135.77	?		2.4
10	3 Aug. 2004	12:02:12	12:02:05	25,450.16	7.41	2.20	4.7
11	4 Aug. 2004	09:32:40	09:32:28	9,895.48	2.56	1.04	2.1
12	4 Aug. 2004	21:46:56		19,303.39	4.25	1.52	2.5
13	5 Aug. 2004	00:45:07		36,742.99	?	3.74	2.3
14	5 Aug. 2004	09:40:24		23,065.03	7.12	1.93	1.7
15	7 Aug. 2004		17:22:24	2,255.69	?	0.23	2.1
16	9 Aug. 2004		16:26:22	17,593.68	3.82	1.38	1.9

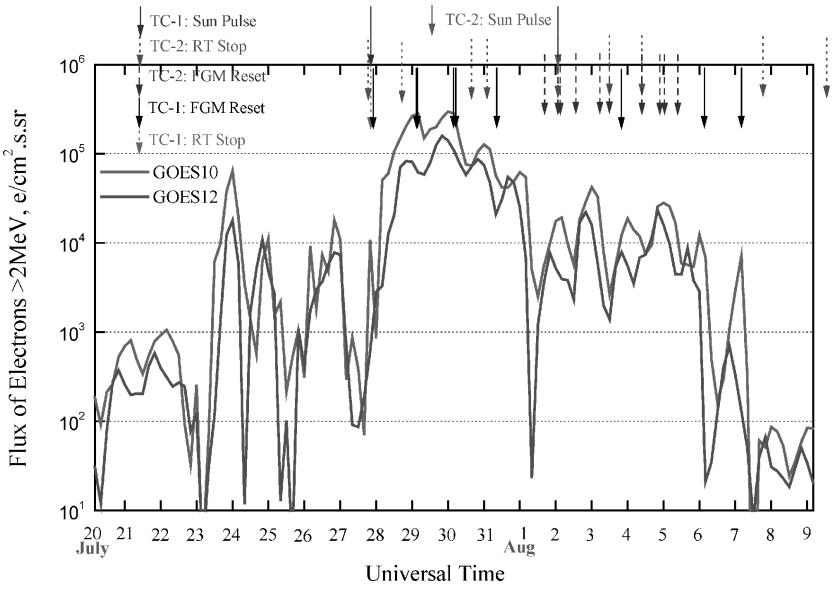

Fig. 1 Hourly averaged flux of penetrating electrons greater than 2 MeV vs time in geosynchronous orbit.

According to the Combined Release and Radiation Effects Satellite (CRRES) experimental result,[8] large ESD may cause more anomalies simultaneously, and the different anomalies taking place within 5 s were treated as caused by a common source. The second point just mentioned indicates that the anomalies are possibly caused by ESD. In addition, the anomalous extra pulses recorded by the sun's pulse sensors on both of the satellites during the interval between two subsequent normal sun's pulses are suspected to be an arcing of ESD. All of these characteristics indicate that ESD produced by internal charging or surface charging may be the cause of the anomalies.

III. Correlation of Anomalies with Penetrating Electron Environment

A great amount of investigations have shown that spacecraft anomalies induced by internal discharging are closely related to enhancement of penetrating electrons. Shown in Fig. 1 are the fluxes of penetrating electrons greater than 2 MeV in geosynchronous Earth orbit (GEO) orbit from 20 July to 10 August, with the data coming from the GOES 10 and 12 satellites. Wrenn and Smith[9] used the daily fluence of 3×10^8 e/cm$^2\cdot$ sr (average flux of 3.5×10^3 e/cm$^2 \cdot$ sr $\cdot$ s) for electrons greater than 2 MeV as the threshold to define enhancements and used a second threshold of

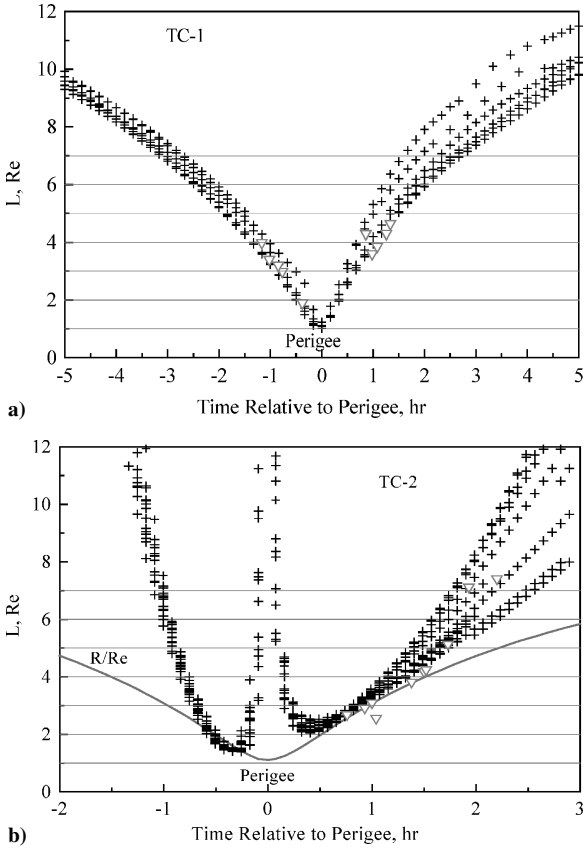

Fig. 2 Orbit showing L value vs time relative to perigee, with orbital locations of events marked by triangles: a) TC-1 and b) TC-2.

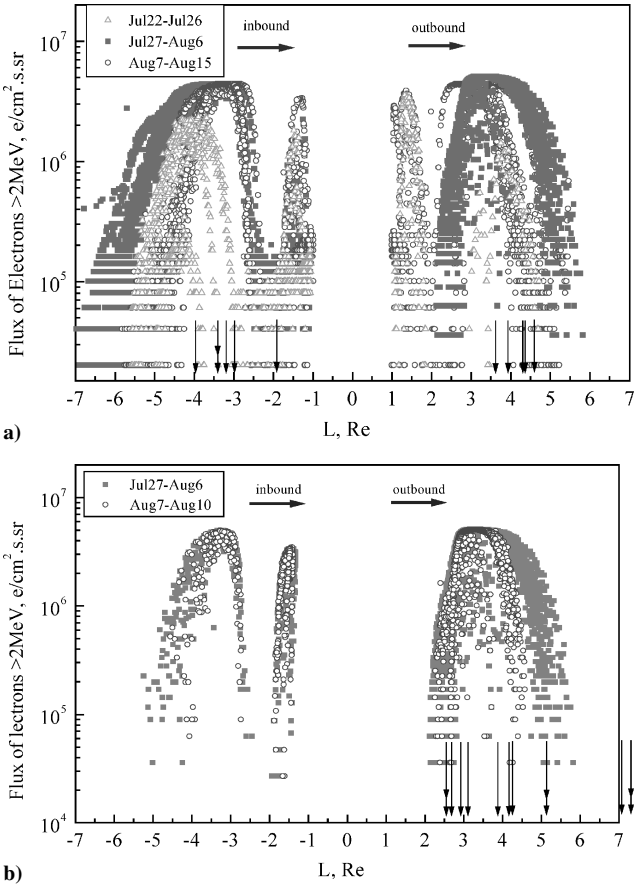

Fig. 3 Flux of electrons greater than 2 MeV experienced by satellites in various L shells, with orbital locations of events marked by arrows: a) TC-1 and b) TC-2.

3×10^9 e/cm$^2 \cdot$ sr (average flux of 3.5×10^4 e/cm$^2 \cdot$ sr $\cdot$ s) to define extreme enhancements. In accordance with this criteria, the high energetic electron flux from 23 July to 6 August reaches the level of enhancement and that between 27 July and 6 August reaches or exceeds the level of extreme enhancement. The anomalies for TC-1 and TC-2 satellites are also marked with arrows in Fig. 1, and it is clear that the majority of anomalies are densely populated during the extreme enhancement, showing good correlation with the penetrating electron environment, which is characteristic of internal discharging induced anomalies.

The penetrating electrons mainly accumulate in the outer radiation belt in the range of $L = 3 \sim 7$; therefore, if the anomalies are caused by internal discharging, they should exhibit a certain pattern of distribution in orbital locations. Figure 2 demonstrates the orbits of the two satellites, showing L value vs time relative to perigee. In Fig. 2, negative hours indicate the inbound side with respect to the perigee and positive hours refer to the outbound side. The orbital locations of events are also marked with signs of an open down triangle. It is clear that most of the anomalies occur in or near the inner and outer radiation belts. However, the occurrence of the anomalies show different characteristics for the two satellites: For TC-1, the events appear on both sides of perigee, whereas for TC-2, the events only occur in the outbound segment instead. All of these characteristics will be explained in the following section.

The two satellites are equipped with a high-energy electron detector (HEED) to monitor the penetrating electron environment in situ. Figure 3 shows the fluxes of electrons greater than 2 MeV experienced by TC-1 (Fig. 3a) and TC-2 (Fig. 3b) in various L shells according to HEED data. In Fig. 3, the negative L values refer to an inbound segment relative to the perigee and the positive refers to the outbound side. From Fig. 3a (TC-1), it can be seen that during the events-populated period, from 27 July to 6 August (solid square points), the distribution of penetrating electrons in the outer radiation belt is increased by around two times and expanded by nearly one Re compared with the previous days (open triangle points), and the peak level is higher than that of GEO locations by more than one order. For the period after 7 August (open circles), the outer radiation belt is narrowed again. For TC-2 (Fig. 3b) the tendency is similar to that of TC-1, although the data before 27 July are lacking.

Hereby, the two satellites experienced much more fluence of penetrating electrons from 27 July to 6 August than the previous and following periods, and, as a result, the majority of anomalies occurred in this interval. Moreover, in the inner radiation belt between $L = 1$ and 2, the flux is also very strong, but the region is much narrower in comparison with the outer belt, and the duration of the spacecraft in this region is much shorter, so that its contribution is much less significant.

The events are also marked by arrows in Fig. 3, and it is clear that the events mostly occur in the region of peak flux level. As shown in Fig. 2, the TC-2 orbit is asymmetric to its perigee, and the satellite does not cross the inner radiation belt in the range of $L \sim 1$–2 when leaving its perigee. That is why HEED failed to detect the flux in the inner radiation belt in the outbound segment, as shown in Fig. 3b.

IV. Instance of Calculation

Whether internal discharges will occur is closely related to the penetrating electron fluence experienced by spacecraft. Violet and Frederickson[5] and Friderickson et al.[8] suggested that a penetrating electron fluence of 1.8×10^{10} electrons/cm^2 was at the threshold for onset of arc discharges. A more recent examination of these data indicated that discharges may occur at lower electron fluence levels, and it was concluded that a firm fluence level below which no discharges occur has not yet been found.[10] Given the possible range of electron fluence values for internal ESD onset and the uncertainties involved, we decided to use the threshold of 2×10^{10} electrons/cm^2 for the moment.

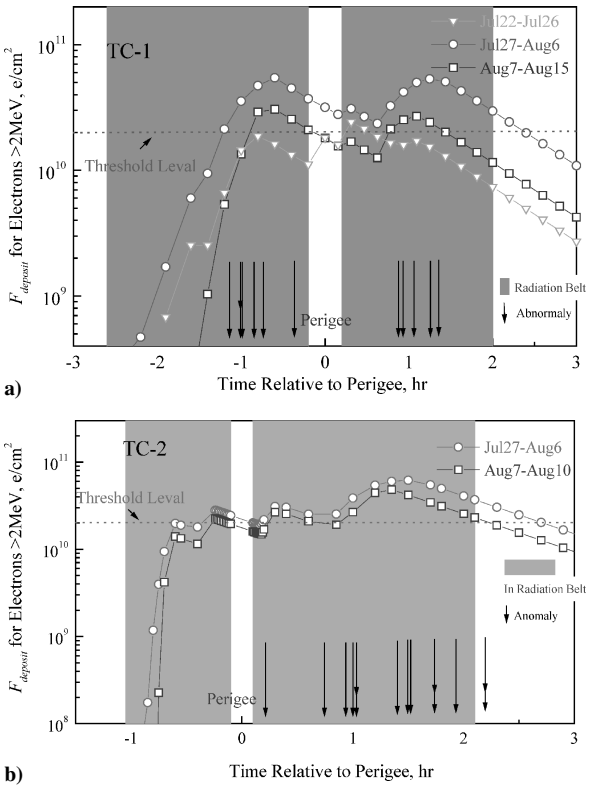

Fig. 4 Integrated flux deposited in dielectrics F_{deposit} for penetrating electrons greater than 2 MeV experienced in orbit vs time relative to perigee: a) TC-1 and b) TC-2.

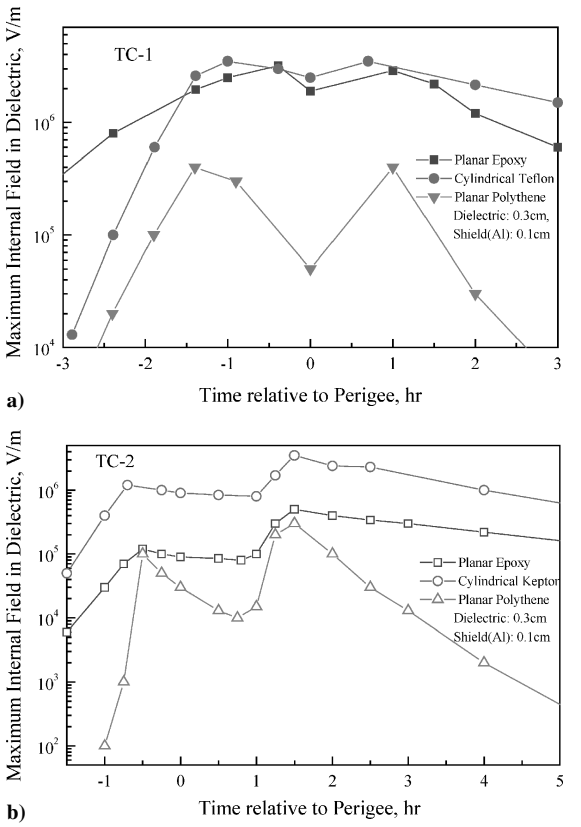

Fig. 5 Maximum internal electric field in some dielectric samples calculated by FLUMIC model vs time relative to perigee: a) TC-1 and b) TC-2.

More precisely, the possibility of discharging is directly related to the number of charges deposited in the dielectrics. Therefore, to evaluate the risk of discharging, we define the integrated flux deposited in dielectrics by F_{deposit}, which is calculated as follows:

$$F_{\text{deposit}}(t + \mathrm{d}t) = F_{\text{deposit}}(t) \cdot \exp(-\mathrm{d}t/\tau) + \text{flux}(t) \cdot \mathrm{d}t \quad (1)$$

where τ is the leakage time constant. As indicated in Eq. (1), the original accumulated charges decrease exponentially due to leakage current. According to the CRRES result,[8] the leakage time constant is between one-half hour and several hours, and here τ is assumed to be 1 h. Although the determination of τ is more or less arbitary, its influence on the result is not significant. The start time for integration is set to be the moment of entering the $L = 7$ shell. Because the satellite has spent many hours under weak electron flux outside the radiation belt before this moment, we assume that the accumulated charges because of a previous crossing of the radiation belt will no longer have an effect, which is also indicated in the literature.[8]

Figure 4 shows the integrated flux F_{deposit} for penetrating electrons greater than 2 MeV experienced in orbit vs time relative to perigee, and the threshold level of 2×10^{10} electrons/cm^2 is shown for comparison. Apparently, all of the anomalies occur in the region with F_{deposit} exceeding the threshold, and the density of events for TC-1 correlate well with the peaks of the integrated flux during the period from 27 July to 6 August. For the previous days (Fig. 4a, open triangle points) and following days (open square points) F_{deposit} is either under the threshold or over the threshold to a less severe degree, which is in good agreement with the fact that both the satellites performed well before 26 July and only one and two anomalies occurred for TC-1 and TC-2, respectively, after 7 August.

Until now, it was possible to find answers to the different characteristics of occurrence for the TC-1 and TC-2 anomalies. As shown in Fig. 2a, the orbit of TC-1 is almost symmetric to the perigee, and it crosses the radiation belt once in the inbound and outbound segments, respectively, with each time lasting about 3 h. During each interval, when the radiation belt was crossed, the integrated flux of penetrating electrons that deposit in the dielectrics is sufficient to produce discharges and lead to anomalies; therefore, the events occur in both the inbound and outbound segments. In contrast, the TC-2 orbit is asymmetric to the perigee as shown in Fig. 2b. (Strictly speaking, the geomagnetic north pole should be used here instead of perigee.) During the crossing of the radiation belt in the inbound side, the duration is less than 1 h, and the experienced integrated flux of penetrating electrons is not sufficient to produce discharges, as shown in Fig. 4b. Whereas for the outbound crossing of the radiation belt, the duration lasts about 2 h, with the additional effect of the previous crossing, the integrated flux exceeds the threshold level very quickly, so that all of the anomalies take place shortly after the satellite's entrance into the radiation belt in the outbound segment.

The more direct way to identify the hazard of discharging is to obtain the electric field in the dielectric victims. Because the victims are unknown, we select some typical dielectric samples with different configurations and calculate the evolvement of their maximum internal electric field during the crossing of the radiation belt, as shown in Fig. 5. The calculation is carried out with DICTAT (URL: http://www.spenvis.oma.be/spenvis [cited 11 January 2004]), and the FLUMIC model[11] is adopted to generate the energy spectrum along the orbits. Because the FLUMIC model cannot reflect the real-time electron flux and give the high energetic electron enhancement during the anomaly days, Fig. 5 only shows the influence of the radiation belt on the evolvement of the internal electric fields in the dielectric samples semiquantitatively. Note that, for TC-1, the peaks of the maximum internal field in the dielectric samples appear symmetrically on both sides of perigee. Instead, for TC-2, the maximum field on the outbound side is apparently higher than on the inbound side. Although the values of the fields are below the suggested breakdown threshold 10^7 V/m due to the application of FLUMIC model instead of real-time energy spectrum, it is clear that for TC-1 the hazards of discharging are similar on both sides of perigee. In contrast, for TC-2, the hazard of discharging on the outbound side is much higher than on the inbound side, which is consistent with both satellites' durations in the radiation belts and their anomaly occurrence patterns.

V. ESD and Electromagnetic Compatibility Tests of RT

To investigate the mechanism leading to RT resets, the responsible group conducted ESD and electromagnetic compatibility (EMC) tests on the spare RT unit. In the ESD test, the sparker was adjusted in a range of frequencies and distances. Even if the distance between the sparker and RT unit was 5 mm, no reset occurred. When the sparker was 20 mm away from the printing circuit board without a cassette, the RT unit reset, but this situation is impossible on the satellite.

In the EMC test, RT reset occurred. The test was conducted in several cases according to MIL-STD-461. In case 1 [MIL-STD-461 CS114 (conducted susceptibility, bulk cable injection, from 10 kHz to 400 MHz)], RT worked well, and no reset or any unusual event occurred. In case 2 [MIL-STD-461 CS116 (conducted susceptibility, damped sinusoidal transients, cable and power leads, from 10 kHz to 100 MHz)], no reset was found at any frequencies except 30 MHz, at which one reset took place. In case 3 [MIL-STD-461 CS115 (conducted susceptibility, bulk cable injection, impulse excitation)], RT reset when the current pulse was over 3.5 A and the frequency of resets increased greatly as the current pulses exceed 5 A. The higher the pulse energy, the more frequent the occurrence of reset. In the worst case, RT was kept in the reset status. If a shielded cable was used instead of the common one, with the two ends of the shield connected to the ground (copper plate), no reset occurred any more. In this experiment, different cables were tested, and the result showed that connecting the shield to the ground firmly kept RT away from resets. Based on the preceding results, the possible cause of RT resets is the high interference pulse conducted from the signal cable into the RT. On the satellite, RT links the instruments without a shielded cable, and some interference pulses on the cable may result from the space environment and lead to RT reset.

VI. Discussion

Although identification of the internal discharging sites and the victim is difficult, even impossible, the correlation of the anomalies with the enhancement of penetrating electrons still presents convincing evidence that internal discharging is the cause of the TC satellites' anomalies. The integrated flux for electrons greater than 2 MeV and a maximum internal electric field for some dielectric samples are also in good agreement with the pattern of occurrence of the anomalies. The ESD and EMC tests of RT also show that the discharging-induced interferences probably coupled into RT units through unshielded cables and resulted in resets. It seems that internal charging is underestimated and that the protection is inadequate, and that precautions may have been taken to protect from its effect.

Surface charging can also produce ESD and lead to spacecraft anomalies, and both TC-1 and TC-2 are equipped with the instrument of active space potential control for monitoring the surface potential in situ; unfortunately, they are turned off during the anomalies. Periods of high surface charging correlate with the peak fluxes of $\sim$30 keV electrons as noted in the literature,[12] but a lack of such flux data prevents us from making further investigations. Studies on surface charging of geosynchronous spacecraft show that the surface charging anomalies are closely related to geomagnetic activity and occur mostly in the local midnight to dawn sector because during magnetic substorms electrons are injected from the local midnight region and drift eastwards.[2] Although the TC-2 events are distributed between local midnight and dawn, TC-1 anomalies occur both in day and night sides, without any revealing tendencies. Therefore, surface charging is unlikely to be the cause of the anomalies.

As for single-event upsets, the possibility is also very small. First, anomalies caused by single-event upsets generally correlate well with the enhancement of high-energy protons and occur mostly in the inner radiation belt; however, during the period of anomalies, the flux of high-energy protons from GOES data did not show apparent enhancement. Second, the error rate produced by single-event upsets is very low, unlikely to result in such dense anomalies within several days. Therefore, the possibility of single-event upsets as a cause can be eliminated.

Acknowledgments

This work was carried out under the support and assistance of many colleagues in the Center for Space Science and Applied Research. The authors would like to especially thank Binsen Xue, Dong Chen, and Qingxiang Zhang for their enthusiastic participation and for providing many helpful suggestions. Sincere thanks are given to Xiaomin Chen for providing the electrostatic discharge and electromagnetic compatibility test results, Jinbin Cao and Jiankui Shi for providing high-energy electron detector data, Xuzhi Li and Chao Shen for help in orbit calculation, as well as to other colleagues for their help.

References

[1]Robinson, P. A., "Spacecraft Environmental Anomalies Handbook," AFGL Publ. GL-TR-89-0222, Hanscom AFB, MA, Aug. 1989.

[2]DeForest, S. E., "Spacecraft Charging at Synchronous Orbit," *Journal of Geophysical Research*, Vol. 77, No. 4, 1972, pp. 651–659.

[3]Gussenhoven, M. S., Hardy, D. A., Rich, F., and Burke, W. J., "High-Level Spacecraft Charging in the Low-Altitude Polar Auroral Environment," *Journal of Geophysical Research*, Vol. 90, No. A11, 1985, pp. 1009–1023.

[4]Garrett, H. B., "The Charging of Spacecraft Surfaces," *Reviews of Geophysics and Space Physics*, Vol. 19, No. 4, 1981, pp. 577–616.

[5]Violet, M. D., and Frederickson, A. R., "Spacecraft Anomalies on the CRRES Satellite Correlated with the Environment and Insulator Samples," *IEEE Transactions on Nuclear Science*, Vol. 40, No. 6, 1993, pp. 1512–1520.

[6]Wrenn, G. L., "Conclusive Evidence for Internal Dielectric Charging Anomalies on Geosynchronous Communications Spacecraft," *Journal of Spacecraft and Rockets*, Vol. 32, No. 3, 1995, pp. 514–520.

[7]Leung, P., Whittlesey, A. C., Garrett, H. B., Robinson, P. A., and Divine, T. N., "Environment-Induced Electrostatic Discharges as the Cause of Voyager 1 Power-On Resets," *Journal of Spacecraft and Rockets*, Vol. 23, No. 3, 1986, pp. 323–330.

[8]Frederickson, A. R., Holeman, E. G., and Mullen, E. G., "Characteristics of Spontaneous Electrical Discharging of Various Insulators in Space Radiation," *IEEE Transactions on Nuclear Science*, Vol. 39, No. 6, 1992, pp. 1773–1782.

[9]Wrenn, G. L., and Smith, R. J. K., "Probability Factors Governing ESD Effects in Geosynchronous Orbit," *IEEE Transactions on Nuclear Science*, Vol. 43, No. 6, 1996, pp. 2783–2789.

[10]Frederickson, A. R., "Methods for Estimating Spontaneous Pulse Rates for Insulators Inside Spacecraft," *IEEE Transactions on Nuclear Science*, Vol. 43, No. 6, 1996, pp. 2778–2782.

[11]Sørensen, J., "An Engineering Specification of the Internal Charging," *Proceedings on Environment Modeling for Space-Based Applications*, ESA SP-392, 1996, pp. 129–138.

[12]Mullen, E. G., Gussehoven, M. S., Hardy, D. A., Aggson, T. A., Ledly, B.G., and Whipple, E., "SCATHA Survey of High-Level Spacecraft Charging in Sunlight," *Journal of Geophysical Research*, Vol. 91, No. A2, 1986, pp. 1464–1490.

A. Ketsdever
Associate Editor